Methylmercury and Amount of Endocytic Activity in Chick Embryonic Glial Cells

Megan L. Donahue
Neurobiology Short Report
Bio324/Neurobiology
Wheaton College, Norton, Massachusetts, USA
April 23, 2014

Introduction:

During the 1970s in the United States, public health threats from methylmercury began (Freeman, 2006). Health concerns were a major issue as methylmercury exposure occurs worldwide and is not limited to isolated populations (Mergler et al., 2007). For instance, all fish contain methylmercury and many occupations expose workers to the toxin (Freeman, 2006) (Mergler et al., 2007). Because this pollutant is plentiful in the environment, humans and other organisms are frequently exposed to it. Methylmercury has negative affects on the nervous system. There is a correlation between methylmercury dosage and specific motor activity and visual functions, hand coordination and muscular fatigue (Lebel et al., 1997). Methylmercury can also cross the blood brain barrier and cause brain damage. In the body's attempt to remove the mercury, divalent mercury can result as a byproduct. This mercury form can accumulate in the kidneys and lead to kidney damage (Griesbauer, 2007). Biomarkers such as hair, fingernails and urine can be utilized to test for the presence of mercury in the body. Hair serves as the most convenient exposure parameter (Mergler et al., 2007). Because methylmercury is highly abundant in the environment and impairs the nervous system, this study was conducted.

Methylmercury is absorbed in the digestive tract and forms a complex with cysteine. This complex closely resembles methionine and can easily be endocytosed (Griesbauer, 2007). Endocytic mechanisms are crucial as they have many roles. They uptake extracellular nutrients, regulate cell-surface receptor expression, and maintain cell polarity and antigen presentation. Unfortunately though, toxins also enter cells using endocytosis (Mukherjee, Ghosh, & Maxfleld, 1997).

Once inside the cell, endosomes' forms change. Upon initial entrance into the cell, early endosomes are formed, specialized vesicles containing one compartment. Ultimately, the endosomes' membranes enfold and a multivesicular endosomes form. Late endosomes are capable of breaking down proteins. The late endosomes fuse to lysosomes and excrete their contents. These lysosomes are required to fully digest the materials that entered the cell during endocytosis (Davidson, 2005).

In this experiment, control and experimental conditions were used. The control condition did not contain any methylmercury, while the experimental condition contained a high dosage of methylmercury. In keeping all other experimental factors the same, the relationship between methylmercury dosage and endocytic activity was studied. In this experiment, we treated chick-sympathetic neurons with methylmercury. Chick embryos of the *Gallus gallus* species were used (R.L. Morris, personal communication, April 2014). Chick embryos were utilized because their dorsal root ganglia and sympathetic nerve chains resemble that of a human, obtaining them is convenient, and 10-day old chicks are unable to experience pain.

The amount of endocytic activity in glial cells treated with varying dosages of methylmercury was studied. Glial cells were investigated as they are the most numerous cell type in the nervous system, outnumbering neurons by a 3:1 ratio (Purves, Augustine, & Fitzpatrick, 2001). Glial cells are crucial in the function of the nervous system as they provide neuronal trophic support, drive nerve fasciculation and modulate axon pathfinding (Freeman, 2006). In this study, we tested the hypothesis that as the dosage of methylmercury increases; the average amount of endocytic activity in glial cells increases as well.

Materials and Methods:

Dissection:

Robert L. Morris' protocol was followed to isolate dorsal root ganglia and sympathetic nerve chains (Morris, 2014a). However, instead of using Hank's Balanced Salt Solution, Dulbecco's Modified Eagle's Medium was used. Additionally, the Flame-construction of Pasteur pipettes step was not performed. To increase the stickiness of the slides, the coverslips were treated with poly-lysine for three hours. To increase cell signaling, the coverslips were treated with laminin for two hours. The NGF (nerve growth factor) concentration was 50-200ng/mL to increase the axon growth rate. The glutamine concentration was 4mM because this amino acid breaks down quickly. In the incubator, the intensity of the vibrations was lessened in order to increase cell adherence. Finally, the dissection occurred 36.5 hours prior to the preparation of the control and experimental conditions.

Control Condition:

A Petri dish containing F-plus growth medium and a coverslip that had been stored in an incubator for 36.5 hours was obtained. Using a Pasteur pipette, the F-plus growth medium was removed from the dish and expelled into a separate, clean dish. DMEM was added to the Petri dish and the Petri dish was placed into the incubator for 20 minutes. The DMEM was removed and put into a waste container. Fresh DMEM was added to wash the Petri dish and coverslip.

Experimental Condition:

A Petri dish containing F-plus growth medium and a coverslip that had been stored in an incubator for 36.5 hours was obtained. The F-plus growth medium was removed using a Pasteur pipette. A 40nM concentration of methylmercury in DMEM was added to the Petri dish. This 40nM concentration was based on an experiment preformed by Leong (Leong, Syed, & Lorschieder, 2001). This methylmercury solution remained in the Petri dish for 20 minutes. The 40nM methylmercury was extracted and deposited into a waste container for mercury. The Petri dish and coverslip were washed again with fresh DMEM.

Endosome Labeling:

The DMEM was removed from the Petri dish. Two milliliters of 10µM fluorescein-dextran in growth medium were added. This fluorescein-dextran concentration was based on a procedure done by Bi and Morris (Bi et al., 1997). 1mL of this solution was added to each Petri dish, the control and the experimental. The fluorescein-dextran solution remained in the Petri dish for 45 minutes, in the incubator. The fluorescein-dextran solution was removed and the coverslip was washed three times with DMEM. A color assay was preformed to ensure that the fluorescein-dextran solution had been removed. Robert L. Morris' protocol was followed to label the endosomes (Morris, 2014c).

Observation Chamber Assembly:

Robert L. Morris' protocol was followed for the assembly of an observation chamber (Morris, 2014b).

Microscopy:

The first prepared slide was placed on the stage of a Nikon Eclipse E200 microscope. The microscope was adjusted for Koehler illumination. The 10X objective lens was used to locate bubbles on the slide. The stage was moved slightly downward and cells came into focus. The objective lens was switched to 40X. With the eyepieces of the microscope, the cell was magnified using transmitted light. The microscope's pin was pulled, which sent the image to the Spot Advanced program on the Macintosh Gemini Computer screen. The "restart" button was pressed and the image appeared. The image of the cell was put into better focus using the fine focus adjustment knob of the microscope. The image was optimized. A photo was taken. The microscope and the Spot Advanced program were then switched to fluorescent mode. The transmitted light was blocked using a think, opaque object. On the Macintosh Gemini Computer, the "fluorescence" and "manual exposure" options were selected. The exposure time was also set at 10 seconds and the gain was set at 2. On the microscope, the slide was adjusted to position 3, the shutter was opened and an image was captured. The photos were saved on the desktop.

Measurement:

Each of the six fluorescence light photos was opened in Adobe Photoshop. The brightness levels were adjusted by the same amount so the green fluorescence portions could be seen more clearly.

The diameter of an endosome was researched to be 200-1000nm (Duzgunes, 1993). Using the line tool in ImageJ, the number of pixels per millimeter was calculated. Every 1µm contained 5.54 pixels. With this information, an endosome was identified in the control condition 1 fluorescence image edited with Adobe Photoshop. The brightness levels were adjusted until the endosome barely appeared. This was the threshold value for an endosome. The same brightness adjustments were made for each of the six images. One glial cell was measured for each image. The approximate number of white pixels in a cell was found. The white pixels represented endocytic activity as they were of the previously determined threshold brightness. The approximate total number of pixels in the glial cell was also measured. The total number of pixels in a glial cell was measured using the transmitted light photos. The number of white pixels and total pixels was measured

using the line tool in ImageJ. The line tool was dragged around the boundaries of the white pixels and the glial cells. In dragging the line tool around the white pixels and glial cells, the number of pixels contained in each was shown on the computer screen.

Data Analysis:

For each glial cell, a ratio of white to total pixels was calculated. This was found by dividing the total number of white pixels by the total number of pixels. The average ratio of white to total pixels in control conditions and the average conditions were calculated. These data were compared and a conclusion was reached in regards to my hypothesis.

Results:

Transmitted light images, fluorescent light images edited with Adobe Photoshop and threshold light images edited with ImageJ were utilized in the collection of my data. Figures 1 and 4 display transmitted light images, which indicate the locations, shapes and sizes of glial cells. The total numbers of pixels located within glial cells were measured in these images. The control condition 1 fluorescent light image edited with Adobe Photoshop, which is shown in Figure 2, was used to classify an endosome. Figure 5 also displays a fluorescence image. Fluorescence images were edited in ImageJ to produce threshold light images, Figures 3 and 6. The numbers of white pixels located within glial cells were measured in these images. Figure 7 displays the average ratios of white to total pixels in glial cells for control and experimental conditions. Six glial cells were analyzed to calculate these averages. As shown by the Figure 7, the ratios of white to total glial cells in control and experimental conditions were relatively the same.

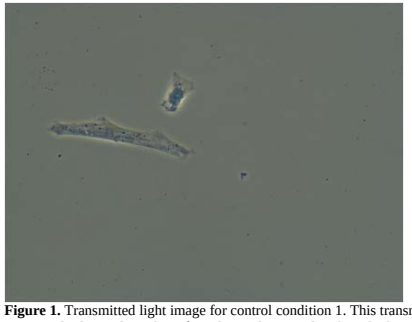

Figure 1. Transmitted light image for control condition 1. This transmitted light photo was used to determine the boundaries, shapes and sizes of the glial cells. Only the long, thin glial cell oriented horizontally on the left side of the image was quantified. In ImageJ, the total number of pixels present in this glial cell was measured. The total number of pixels was later used in the calculation of the ratio of white to total pixels. I captured this image with Dana MacDonald and Gabriella Verde.

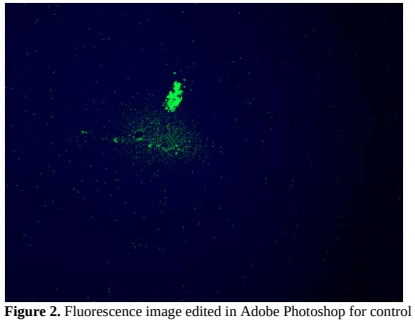

Figure 2. Fluorescence image edited in Adobe Photoshop for control condition 1. In this image, 1µm contains 5.54 pixels. This image was used to determine which neon spot represented an endosome. I edited this photo with Dana MacDonald and Gabriella Verde.

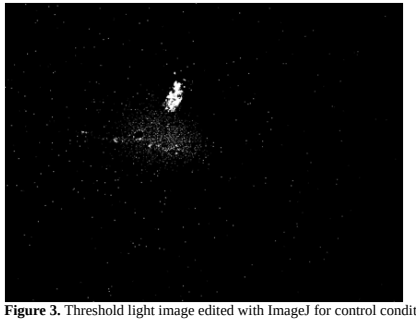

Figure 3. Threshold light image edited with ImageJ for control condition 1. This image was used to measure the white pixels located within a glial cell. Dana MacDonald and I captured this image together; however, we quantified our data separately.

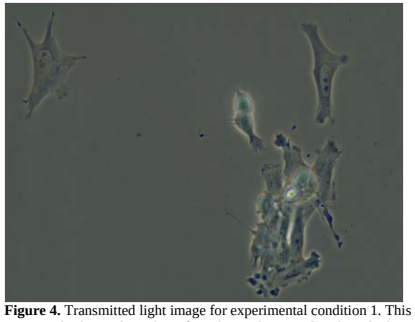

Figure 4. Transmitted light image for experimental condition 1. This transmitted light photo was used to determine the boundaries, shapes and sizes of the glial cells. Only the large glial cell located in the bottom right-hand corner of the image was quantified. In ImageJ, the total number of pixels present in this glial cell was measured. The total number of pixels was later used in the calculation of the ratio of white to total pixels. Dana MacDonald, Gabriella Verde and I captured this image together, and Gabriella displayed the image in her lab report as well.

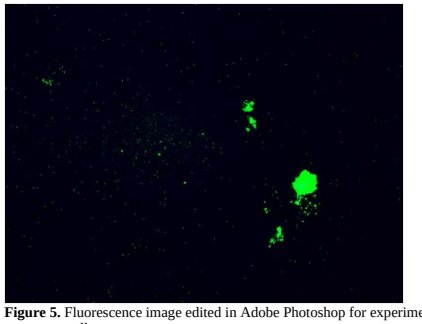

Figure 5. Fluorescence image edited in Adobe Photoshop for experimental condition 1. This fluorescence image was edited in ImageJ in order to achieve the threshold light image, which is shown in Figure 6. Dana MacDonald, Gabriella Verde and I captured this image together, and Gabriella displayed this image in her lab report as well.

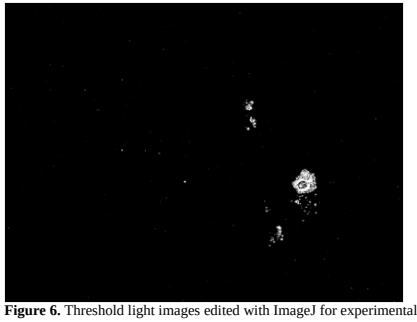

Figure 6. Threshold light images edited with ImageJ for experimental condition 1. This image was used to measure the white pixels located within a glial cell. Dana MacDonald and I captured this image together; however, we quantified our data separately.

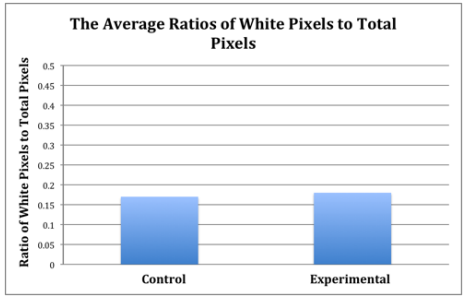

Figure 7. The average ratio of white pixels to total pixels in glial cells (n=6 glial cells). Dana MacDonald, Gabriella Verde and I shared transmitted light and fluorescence images edited with Adobe Photoshop. Dana MacDonald and I shared threshold images. Although I shared data and collaborated with these researchers, I measured and calculated the ratios of white pixels to total pixels independently.

Discussion and Conclusions:

The hypothesis that, as methylmercury dosage increases, the average amount of endocytic activity in glial cells increases as well, is rejected. If endocytic activity were to increase, then a greater ratio of white pixels to total pixels would have been measured. The average ratios of white pixels to total pixels in control and experimental conditions were relatively the same, 0.17 and 0.18.

In endocytosis, endosomes enter the cell through the invagination of the cell's plasma membrane to surround macromolecules and other foreign materials in the extracellular matrix (Davidson, 2005). Matter enters the cell in the pinching off of the plasma membrane, in a process known as budding (Davidson, 2005). The macromolecules are released into the cell's cytoplasm in vesicles called endosomes. These endosomes then travel to lysosomes, where their inner contents are digested and destroyed (Davidson, 2005).

Similarly to other foreign materials, when methylmercury is present in the extracellular matrix, it is endocytosed (Davidson, 2005). The presence of methylmercury in the extracellular matrix does not affect endocytic activity. Endocytosis will continue to occur in cells regardless of which compounds surround the cell. Therefore, if methylmercury is added to the extracellular matrix, the amount and rate of endocytic activity is not affected (Battey, James, Greenland, & Brownlee, 1999). Rather, the only difference is which foreign materials enter the cell. If methylmercury is present in the extracellular matrix, then it is endocytosed. If methylmercury is not present in the extracellular matrix, then other macromolecules and foreign materials are endocytosed.

There was a source of error in our experiment. In experiments, it is crucial that control and experimental conditions remain constant, except for the independent variable. In this study, the independent variable was the presence of methylmercury. However, in the microscopy portion of the procedure, an inconsistency occurred. The images for the control condition slide were captured immediately after the preparation of the slides. The images for the experimental condition slide were not captured until about an hour had passed. Because the cells were alive, endocytosis was likely occurring during this time period. In order to eliminate this inconsistency between control and experimental conditions in future experiments; two different sets of microscopes and computers should be utilized in the capturing of the images. This would allow both conditions to be captured simultaneously. This procedural modification would prevent time from serving as a factor (D. MacDonald, personal communication, April 2014).

Prior research on the relationship between methylmercury dosage and endocytic activity has not been published. Endocytic activity in glial cells is an important topic to study though because methylmercury is highly abundant in the environment and the toxin negatively affects the nervous system (Davidson, et al. 1998). In order to reduce the effects of the toxin on the nervous system, the mechanism by which the toxin is removed from our cells should be studied. This research could improve the health sciences.

In regards to future experiments, the relationship between toxins other than methylmercury and endocytic activity should be studied. Experimentation with other toxins could provide insight as to whether or not toxins in general affect endocytic activity in glial cells. Additionally, the relationship between methylmercury dosage and endocytic activity in neurons could be studied. It would be interesting to investigate whether or not endocytic activity is similar in all cell types. A deeper understanding of the mechanism by which methylmercury affects the nervous system, and furthermore organisms, could be obtained.

References Cited:

Battey, N., James, N., Greenland, A., Brownlee, C. (1990). Exocytosis and Endocytosis. Retrieved from: http://www.plantcell.org/content/11/4/643.full

Bi, G. Q., Morris. R. L., Liao, G. Alderton, J. M., Scholey, J. M., & Steinhardt, R.A. (1997). Kinesin-and myosin-driven steps of vesicle recruitment for Ca2+ regulated exocytosis. *The Journal of Cell Biology, 138 (5), 999-1008*. Retrieved from: http://jcb.rupress.org/content/138/5/999.long.

Davidson, M.W. (2005). Endosomes and Endocytosis. Molecular Expressions CellBiology. Retrieved from: http://micro.magnet.fsu.edu/cells/endosomes/endosomes.html.

Duzgunes, N. (1993). Membrane Fusion Techniques. Retrieved from: http://books.google.com/books?id=K9LyXYS8IREC&pg=PA220&lpg=PA220&dq=diameter+of+an+endosome+1000+nm&source=bl&ots=usHL8udP62&sig=YAN9949nCn_GgLFg6GKMJYmU4YE&hl=en&sa=X&ei=zAVXU5KYFZfJsQSw3oLQCw&ved=0CEkQ6AEwBA#v=onepage&q=diameter%20of%20an%20endosome%201000%20nm&f=false.

Freeman M.R. (2006). Sculpting the nervous system: glial control of neuronal development. Science Direct. DOI: 10.106/j.conb.2005.12.004

Griesbauer, L. (2007). Methylmercury Contamination in Fish and Shellfish. *ProQuest*. Retrieved from: http://www.csa.com/discoveryguides/mercury/review4.php.

Lebel, J., Mergler, D., Branches, F., Lucotte, M., Amorim, F. and Dolbec, J. (1998). Neurotoxic Effects of Low-Level Methylmercury Contamination in the Amazonian Basin. Retrieved from: http://www.ncbi.nlm.nih.gov/pubmed/9756677.

Leong, C.C., Syed, N.I., & Lorschieder, F.L. (2001). Retrograde degeneration of neurite membrane structural integrity of nerve growth cones following in vitro exposure to mercury. *Neuroreport, 12 (4), 733-737*. Retrieved from: http://www.ncbi.nlm.nih.gov/pubmed/11277574.

MacDonald, D. Personal Communication, April 2014.

Mergler, D., Anderson, H., Chan, L., Mahaffey, K., Murray, M., Sakamoto, M. and Stern, A. (2007). Methylmercury Exposure and Health Effects in Humans: A Worldwide Concern. BioOne. http://dx.doi.org/10.1579/0044-7447(2007)36[3:MEAHEI]2.0.CO;2

Morris, R.L. (2014a). Neurobiology Bio324 Primary Culture Of Chick Embryonic Peripheral Neurons 1: DISSECTION. Retrieved from: http://icuc.wheatoncollege.edu/bio324/2014/morris_robert/BIO324_Lab_Proc_1_Dissecti on_2014.htm.

Morris, R.L. (2014b). Neurobiology Bio324 Primary Culture Of Chick Embryonic Peripheral Neurons 2: OBSERVATION of LIVE UNLABLED CELLS. Retrieved from: http://icuc.wheatoncollege.edu/bio324/2014/morris_robert/BIO324_Lab_Proc_2_ObserveLiveCells_2014.htm

Morris, R.L. (2014c). Neurobiology Bio324 Primary Culture Of Chick Embryonic Peripheral Neurons 3: STAINING and OBSERVATION of LIVE CELLS. Retrieved from: http://icuc.wheatoncollege.edu/bio324/2014/morris_robert/BIO324_Lab_Proc_3_StainAndObserv_2014.htm.

Morris, R. Personal Communication, April 2014.

Mukherjee S., Ghosh R.N., Maxfield F.R. (2007). American Physiological Reviews Retrieved from: http://physrev.physiology.org/content/77/3/759.

Purves, D., Augustine G.J., Fitzpatrick D. (2001). *Neuroglial Cells*. Neuroscience – NCBI Bookshelf. Retrieved from: http://www.ncbi.nlm.nih.gov/books/NBK10869/.

Verde, G. Personal Communication, April 2014.

I have abided by the Wheaton College Honor Code in this work.
Megan L. Donahue